

CFD Simulation of Air Cyclone Separator

Nuha wathq Nema¹Saad Nahi Saleh²Fayadh Mohamed Abed³^{1,2}Chemical Engineering Department, Tikrit University, Salahaldeen, Iraq³Mechanical Engineering Department, Tikrit University, Salahaldeen, Iraq

Abstract

A computational fluid dynamics model was developed for air cyclone separator in order to predict the flow pattern inside the cyclone using an Eulerian approach, three dimensions Reynolds-Average Navier-Stokes equations, closed via the Reynolds Stress model as a turbulence model for air flow. The particles were modeled as a discrete phase model using the Lagrangian transport model with turbulent particle dispersion. Computational fluid dynamics modeling was employed to investigate fluid flow patterns and particle trajectories at steady state operating conditions of Stairmand cyclone. Analysis of a computational fluid dynamics simulation accurately revealed that the air flow behavior in cyclone separator consists of two vortices: an outer vortex with a downwardly directed axial flow and an inner vortex with an upwardly directed flow, this flow profile known as Rankine vortex. A low-pressure zone appeared in the center line of the cyclone due to high swirling velocity. The results showed that the pressure drop increased with increasing the inlet air velocity. The results of the collection efficiency showed that the efficiency increased as the particles diameter increased. A good agreement achieved between the simulation results and published experimental results. The computational fluid dynamics code (ANSYS FLUENT 14.5) with the Reynolds Stress model as the turbulence model, predicted very well the flow field parameters of cyclones and can be used in cyclone design for any dimensions.

Keywords: CFD, Cyclone Separator, Lagrangian transport model, Rankine vortex.

المحاكاة باستخدام ديناميكية الموائع الحسابية لفرازة الهواء الدوامية

الخلاصة

ان نموذج ديناميكية الموائع الحسابية (Computational Fluid Dynamics) استخدم لوصف سلوك فرازة الهواء الدوامية (السايلكون) من اجل فهم افضل لسلوك الجريان داخل السايلكون باستخدام تقريب أوليبر (Eulerian approach) وباستخدام نموذج ثلاثي الابعاد ومعدل رينولد لمعادلات نافير ستوك ونموذج اجهاد رينولد لوصف الاضطراب في جريان الهواء، واستخدم نموذج (Discrete Phase Model) لوصف سلوك الطور الصلب باستخدام نموذج لاكرانج للانتقال مع تشتيت الدقيقة المضطرب. ان النمذجة باستخدام ديناميكا الموائع الحسابية استعملت لوصف اسلوب جريان الغاز داخل السايلكون، واسلوب التأثير بين الدقائق الصلبة والغاز تحت ظروف تشغيل الحالة المستقرة لسايلكون ستيرماند (Stairmand cyclone). أظهرت نتائج المحاكاة وبدقة عالية بأن سلوك التدفق الهوائي في السايلكون يتكون من دوامتين وهي: دوامة خارجية مع اتجاه تدفق محوري نحو الاسفل ودوامة داخلية مع اتجاه تدفق نحو الاعلى، ان اسلوب التدفق هذا يعرف بدوامة رانكن (Rankine vortex). كذلك فان منطقة ضغط منخفضة ظهرت في الخط المركزي للسايلكون بسبب السرعة الدوارة العالية. أظهرت النتائج كذلك بأن هبوط الضغط زاد بزيادة سرعة الهواء الداخلة. ان نتائج كفاءة الفصل أظهرت بأن الكفاءة زادت بزيادة قطر الجزيئات الصلبة. كذلك جاءت نتائج المحاكاة مقارنة جدا للبيانات التجريبية المنشورة. ان البرنامج المعتمد على ديناميكا الموائع الحسابية (ANSYS FLUENT 14.5) مع نموذج إجهاد رينولد لوصف الاضطراب في جريان الهواء، تنبأ بعوامل مجال الجريان للسايلكون بصورة جيدة جدا وبذلك ممكن استخدامه لوصف سلوك السايلكون لأي تصميم.

الكلمات الدالة: ديناميكية الموائع الحسابية، فرازة الهواء الدوامية، نموذج لاكرانج للانتقال، دوامة رانكن.

Introduction

Cyclone separators are the most popular cleaning devices used in the industry to separate discrete particles from continuous phase[1].

In spite of their simple structure the fluid dynamics and flow behavior in a cyclone separator are very complex. The complexity of the cyclones is due to the extreme complexity of the swirling turbulent flow field inside the device, strong anisotropy and possible non stationary features typical of highly swirling motions. Until this day and after more than a century of research the flow inside cyclone separator is not completely understood [2-5].

Cyclones may be designed as either classifiers or separators with a wide range of applications. Examples include their use in the separation or classification of plastic fines, sawdust, plastic and metal pellets, rock and mineral crushing, and catalyst and petroleum coke fines[6].

The basic principle of the cyclone is to separate solid particles from a moving gas stream without the use of moving mechanisms or filters. The shape and structure of the cyclone body generates an internal air vortex, where inertia and gravitational forces effect particle separation [7,8].

The most commonly used design is the reverse-flow cyclone which is shown in Figure (1)[4].The gas and the solid particles forced through a tangential inlet at the upper part of the cyclone. The tangential inlet produces a swirling motion of gas, which causes the particles to move toward the cyclone wall and then the solid particles leave the cyclone through a duct at the base of the apex of the inverted cone while the gas swirls upward in the middle of the cone and leaves the cyclone from the vortex finder, this flow pattern is often called a 'double vortex': an outer vortex with downwardly directed axial flow and an inner one with upwardly directed flow [2,6,9].

The Computational Fluid Dynamics (CFD) is very useful method in the field of studying the cyclone behavior without actually building the real physical model. In 1982 Boysan et al. was the first who introduced the Computational Fluid Dynamics (CFD) principles in the field of flow simulation of cyclones. From that time many researchers continued this work and utilized the CFD technique and experimental

work to improve the construction and operation of cyclones due to their advantages and widely applications[10]. From an engineering point of view, cyclone performance is measured by pressure drop and collection efficiency. A criterion for comparing the collection efficiency of cyclones is the cut-off diameter (D_{50}). The cut-off diameter is the diameter of particle which has (50%) probability of separation and (50%) probability of escaping [8,11].

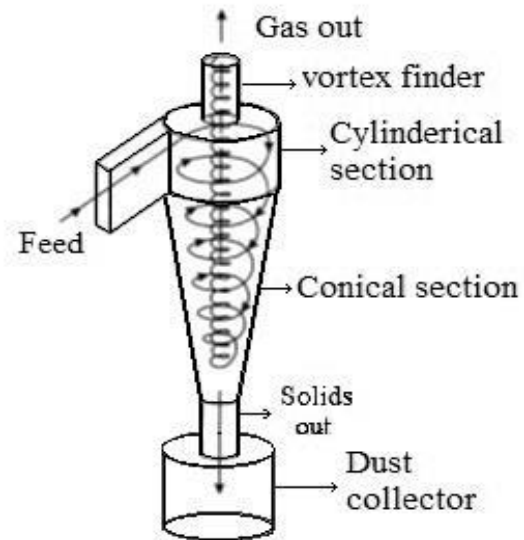


Fig. 1. Sketch of the Reverse-flow cyclone[4]

The purpose of this study is investigating fluid flow patterns, and particle trajectories at steady state operating conditions of Stairmand cyclone. The effect of the inlet velocity on the pressure drop are quantified.

The Computational Fluid Dynamics (CFD) is very useful method in the field of studying the cyclone behavior without actually building the real physical model. In 1982 Boysan et al. was the first who introduced the Computational Fluid Dynamics (CFD) principles in the field of flow simulation of cyclones. From that time many researchers continued this work and utilized the CFD technique and experimental work to improve the construction and operation of cyclones due to their advantages and widely applications [10]. From an engineering point of

view, cyclone performance is measured by pressure drop and collection efficiency. A criterion for comparing the collection efficiency of cyclones is the cut-off diameter (D_{50}). The cut-off diameter is the diameter of particle which has (50%) probability of separation and (50%) probability of escaping [8, 11].

The purpose of this study is investigating fluid flow patterns, and particle trajectories at steady state operating conditions of Stairmand cyclone. The effect of the inlet velocity on the pressure drop are quantified.

Mathematical Modeling

The governing equations of fluid flow represent mathematical statements of the conservation laws of the mass of a fluid is continuity equation (Equation (1)), and the rate of momentum change is Navier-Stock equation (Equation (2)), which equals the sum of the forces on a fluid particle (Newton's second law)[12]:

$$\frac{\partial u_i}{\partial x_i} = 0 \dots\dots\dots(1)$$

$$\frac{\partial u_i}{\partial t} + u_j \frac{\partial u_i}{\partial x_j} = - \frac{1}{\rho} \frac{\partial P}{\partial x_i} + \frac{1}{\rho} \frac{\partial \tau_{ji}}{\partial x_j} \dots\dots\dots(2)$$

The viscous stresses [τ_{ij} ($x_{i,j}$, t)] is defined by $\tau_{ij} = 2\mu s_{ij}$ where μ is the molecular viscosity and s_{ij} is the strain rate tensor defined by Kegg[13]:

$$s_{ij} = \frac{1}{2} \left(\frac{\partial u_i}{\partial x_j} + \frac{\partial u_j}{\partial x_i} \right) \dots\dots\dots(3)$$

According to the Reynolds explanation the instantaneous velocity may be expressed as the sum of mean and fluctuating components, in general, this can be written as:

$$u_i = U_i + \hat{u}_i \dots\dots\dots(4)$$

Substituting Equation (4) in (2) and make some arrangement, the Reynold- averaged Navier-Stokes (RANS) equation obtained which is:

$$\rho \frac{\partial U_i}{\partial t} + \rho U_j \frac{\partial U_i}{\partial x_j} = - \frac{\partial P}{\partial x_i} + \frac{\partial}{\partial x_j} (2\mu S_{ji} - \rho \overline{u'_j u'_i}) \dots\dots(5)$$

Where the term $-\overline{\rho \hat{u}_i \hat{u}_j}$ is the Reynolds- stress tensor. To compute the $-\overline{\rho \hat{u}_i \hat{u}_j}$, the Reynolds Stress model (RSM) used in this research as a turbulent model. The form of the RSM model is:

$$\frac{\partial}{\partial t} (\rho \overline{u'_i u'_j}) + C_{ij} = D_{T,ij} + D_{L,ij} + \dots\dots\dots(6)$$

$$P_{ij} + \phi_{ij} - \varepsilon_{ij} + F_{ij} + S\phi$$

Where:

$$C_i = \frac{\partial}{\partial x_k} (\rho u_k \overline{\hat{u}_i \hat{u}_j}) \dots\dots\dots(7)$$

$$D_{L,ij} = \frac{\partial}{\partial x_k} \left[\mu \frac{\partial}{\partial x_k} (\overline{\hat{u}_i \hat{u}_j}) \right] \dots\dots\dots(8)$$

$$P_{ij} = -\rho (\overline{\hat{u}_i \hat{u}_k} \frac{\partial u_j}{\partial x_k} + \overline{\hat{u}_j \hat{u}_k} \frac{\partial u_i}{\partial x_k}) \dots\dots\dots(9)$$

$$F_{ij} = -2\rho \Omega_k (\overline{\hat{u}_j \hat{u}_m} \varepsilon_{ikm} + \overline{\hat{u}_i \hat{u}_m} \varepsilon_{jkm}) \dots\dots(10)$$

$$D_{T,ij} = - \frac{\partial}{\partial x_k} \left[\rho \overline{\hat{u}_i \hat{u}_j \hat{u}_k} + \overline{P (\delta_k \hat{u}_i + \delta_{ik} \hat{u}_j)} \right] \dots\dots(11)$$

$$\phi_{ij} = P \left(\frac{\partial \hat{u}_i}{\partial x_j} + \frac{\partial \hat{u}_j}{\partial x_i} \right) \dots\dots\dots(12)$$

$$\varepsilon_{ij} = 2\mu \frac{\partial \hat{u}_i}{\partial x_k} \frac{\partial \hat{u}_j}{\partial x_k} \dots\dots\dots(13)$$

The constants are $\sigma_k = 0.82$, $C_\mu = 0.09$, $\sigma_\varepsilon = 1.0$, $C_{\varepsilon_1} = 1.44$, $C_{\varepsilon_2} = 1.92$, $Pr_t = 0.85$, $C_1 = 1.8$, $C_2 = 0.6$, $C_3 = 0.5$, $C_4 = 0.3$, $C_5 = 0.392$.

The Eulerian-Lagrangian approach was used to calculate the particle trajectories in the flow. The equation of motion for an individual particle can be written as:

$$\frac{du_p}{dt} = \frac{18 \mu C_D Re}{\rho_p d_p^2} (u - u_p) + \frac{g(\rho_p - \rho)}{\rho_p} \dots\dots(14)$$

Where: Re is the relative Reynolds number

$$Re = \frac{\rho d_p |u_p - u|}{\mu} \dots\dots\dots(15)$$

C_D is the drag coefficient computed for spherical particles as the correlations developed by Morsi and Alexander [14]:

$$C_D = a_1 + \frac{a_2}{Re} + \frac{a_3}{Re^2} \dots\dots\dots(16)$$

The constants a_1 , a_2 and a_3 are 0.6167, 46.5 and -116.67 respectively.

Simulation Work

The Stairmand cyclone of 0.2m in diameter, that shown in Figure (2), was used to study in this research. It is a reverse flow device with a tangential inlet, and is often used for industrial gas cleaning. It is considered by seven dimensions that are frequently expressed as their ratio to the cyclone body diameter (D)[15,16]. Where $a/D=0.5$, $b/D=0.2$, $De/D=0.5$, $H/D=4.0$, $h/D=1.5$, $S_v/D=0.5$ and $B/D=0.375$. Table (1) shows the dimensions of the cyclone separator that used in this research.

The general steps for the simulation process through using CFD technique are a building the geometric model, meshing the geometric model, applying the boundary conditions, computational analysis and visualization the results. GAMBIT software used to build the model of cyclone separator. The meshing of cyclone geometry was generated using ANSYS workbench 14.5. Also the modeling and analysis was solved by using Fluent 14.5.

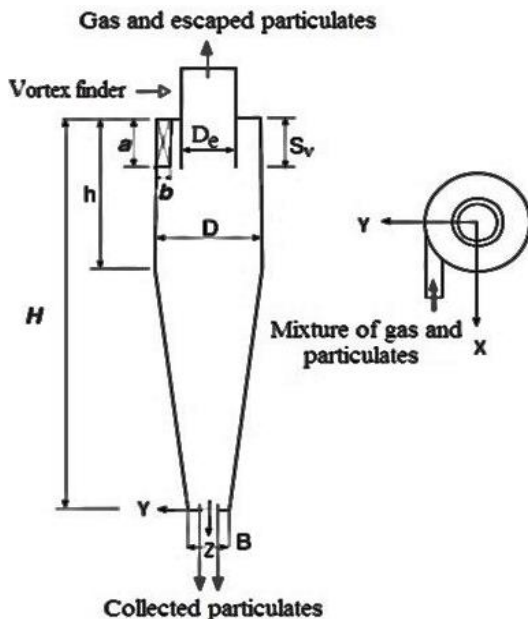


Fig. 2. Stairmand high efficiency cyclone[16]

Table 1. Dimensions of the cyclone separator

Geometric data	Dimensions (m)
D	0.2
De	0.1
B	0.075
H	0.8
h	0.3
S	0.1
a	0.1
b	0.04

Mesh Generating

One of the most important steps in the simulation of the cyclone separator is the mesh or grid generation which mean subdivided of the domain into a number of smaller subdomains in order to solve the flow problems within the created domain geometry.

The accuracy of a CFD solution is strongly governed by the number of cells in the mesh within the computational domain. In general, the larger number of cells is the better accuracy of the solution, but the cost of computer hardware and calculation time are increased[17, 18]. Finer meshes in the near wall region and coarser meshes in other regions are applied in order to obtain the best results with lower cost. Figure (3) shows the cyclone geometry meshing with unstructured mesh type. The total numbers of elements were 386149 and the total numbers of nodes were 129213.

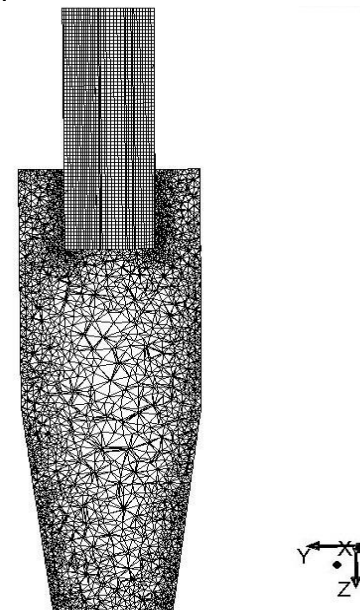


Fig. 3. Cyclone geometry meshing

Boundary Condition

The boundary conditions of inflow velocities at the cyclone inlet were assumed to be uniform. The Discrete Random Walk (DRW) model was used for including the effect of instantaneous turbulent velocity formulations on the particle trajectories. The outlet boundary condition was set at atmospheric pressure and the nonslip boundary condition was used at all walls. The boundary conditions for the solid phase were (the flowing velocity=1m/s, the mass flow rate=0.001kg/sec and the volume fraction= 4.0×10^{-5}). For the gas phase, the inlet were (the inlet velocity=10m/s and the flow rate= $4\text{m}^3/\text{s}$). The air physical properties are (density= $1.225\text{Kg}/\text{m}^3$, viscosity= $1.7894\text{e-}5\text{ Kg}/\text{m}$. and temperature= 298.15k). Where the physical properties of the solid particles are (the diameter rang=(5–200) μm , mean diameter= $85\mu\text{m}$, density= $1200\text{kg}/\text{m}^3$ and spread parameter=2.8).

Solution procedure

The governing equations that expressed above, Equations (1–13), were solved numerically using the commercial CFD code (ANSYS FLUENT 14.5), in which the finite volume method was used to discretize the transport equations. The pressure-velocity coupling algorithm SIMPLEC (SIMPLE Consistent) and the higher upwind interpolation scheme were used in the numerical calculation. A steady-state run was performed and the numerical experiments were carried out with an accuracy of 10^{-4} .

The size of the particles fed is not uniform but follows a continuous distribution over a wide range of particles diameter. The Rosin-Rammler model was used to described the distribution size of the particles in a cyclone separator. Discrete Random Walk (DRW) model used to include the effects of turbulence on the particle dispersion. The Lagrangian approach was used to study the phase dispersed particle trajectory.

Results and Discussion

In this section, the flow behavior of the cyclone (Tangential velocity, Axial velocity and pressure drop) was shown here. Also, the particle trajectory and the collection efficiency of the cyclone were performed. The data were

specified at a vertical plane and at $Z=0.0$, 0.3 , 0.5 , and 0.8 m from the top outlet of the cyclone, as shown in Figure (4)

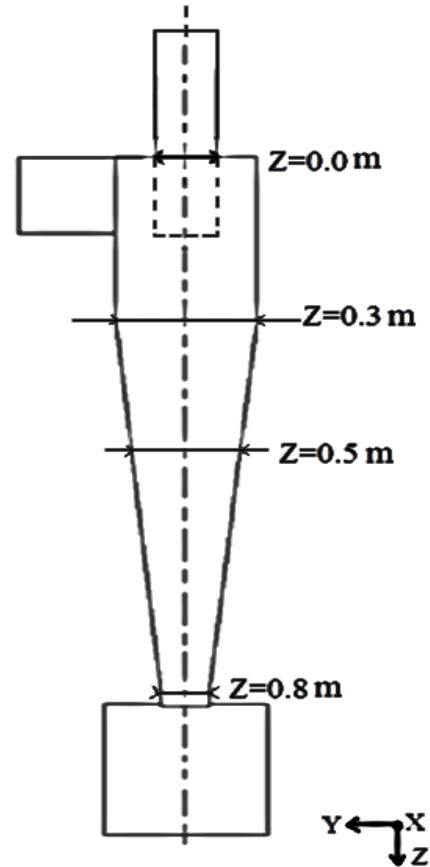


Fig. 4. Sketch of the cyclone with the measurement vertical levels in (m)

Velocity Field Behavior

Figure (5) shows the contour of tangential velocity at a vertical plane of Stairmand cyclone where the maximum value of the tangential velocity occurred at a region between the wall and the core of rotating flow, then it begun to decrease at the center of cyclone to be very low at the axis. This flow behavior known as a Rankine vortex type, including a quasi-forced vortex in the central region and a quasi-free vortex in the outer region. The maximum value of the tangential velocity was 14.3m/s. The result gives an indications that the maximum tangential velocity was about 1.4 times the air inlet velocity.

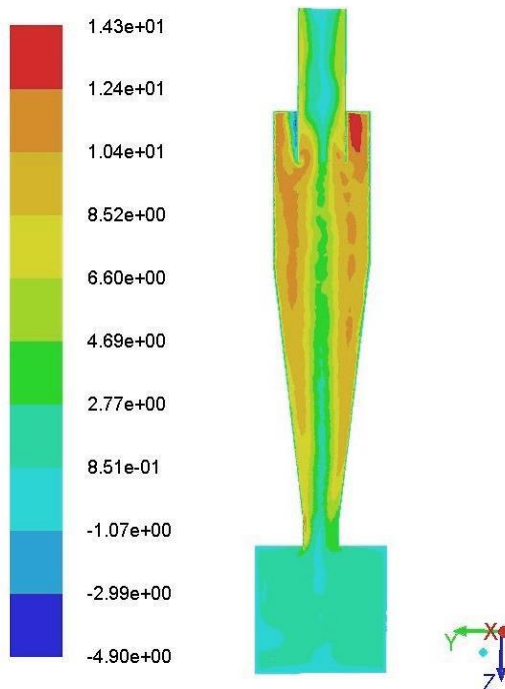


Fig. 5. Contour of tangential velocity at a vertical plane of Stairmand cyclone at air inlet velocity 10m/s

From contours of an axial velocity, Figure (6), at near wall region a high axial velocity appeared and the depression in the value of the axial velocity was clearly visible in region near the axis of the cyclone. The maximum value of the axial velocity was 9.42m/s. The results show that the maximum value of the axial velocity was 0.78 times the air inlet velocity.

The tangential velocity profiles, Figure (7), show that the swirling flow inside the cyclones consists of two regions: an outer free vortex and an inner forced vortex in the center. This phenomena known as a Rankine vortex type. The profiles of tangential velocity were rather similar at different sections. Also, the results show that the tangential velocity distribution varied only slightly with axial positions for the cyclone. This indicates that, if the tangential velocity increases at one section of the cyclone, the same increasing is happened at all other sections.

The Axial velocity profiles, Figure (8), show that near the wall the flow directed downwards the cyclone (positive direction of z-axis) and at the center the flow directed upwards the vortex finder exit(negative direction of z-axis). From the axial velocity plots, the wall moves inward when moves down the cyclone. Also, the results show that the axial velocity decreased in the conical section of the cyclone as the axial position increased due to decreasing in the radial of the cone. At all sections the axial velocity profile was followed the W-shaped profile which it represent an axial velocity profile with minimum of axial velocity at the vortex core.

For CFD validation, a comparisons between Simulation data of Stairmand cyclone and an published experimental data[19] was performed in terms of tangential and axial velocities at (Z=0.17m) and at air inlet velocity of 20m/s. A good agreement achieved between the simulation results and experimental results as shown in Figures (9) and (10) with a deviation of about 15% for tangential velocity and 10% for axial velocity from experimental data.

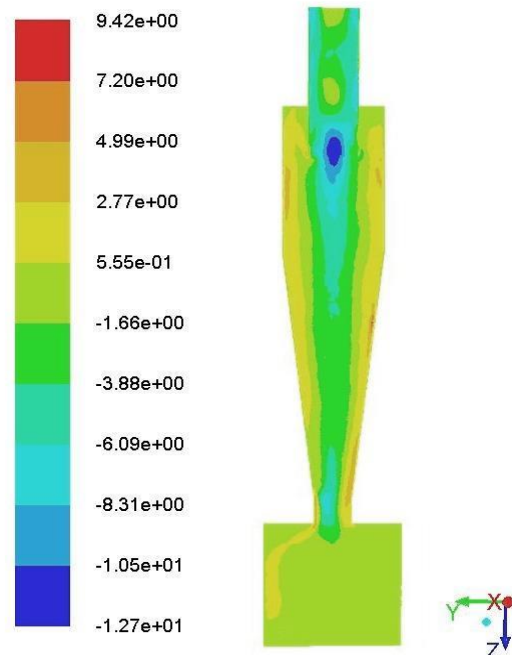


Fig. 6. Contour of axial velocity at a vertical plane of Stairmand cyclone at air inlet velocity 10m/s

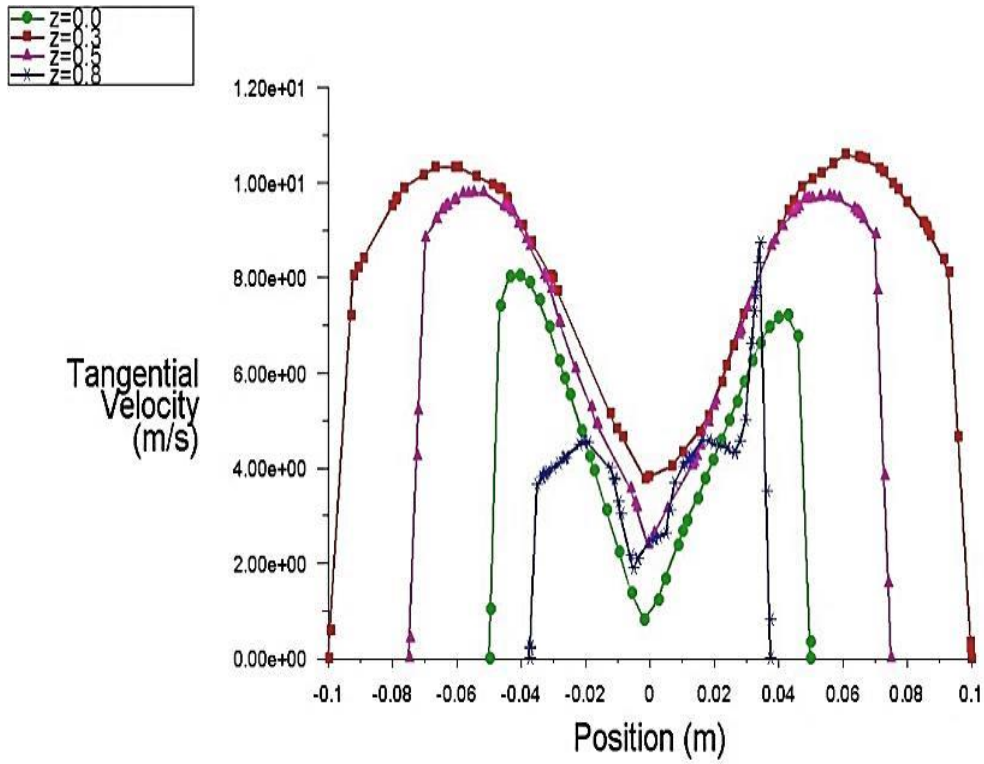


Fig. 7. Tangential velocity at a series of vertical stations in a Stairmand cyclone at air inlet velocity of 10m/s

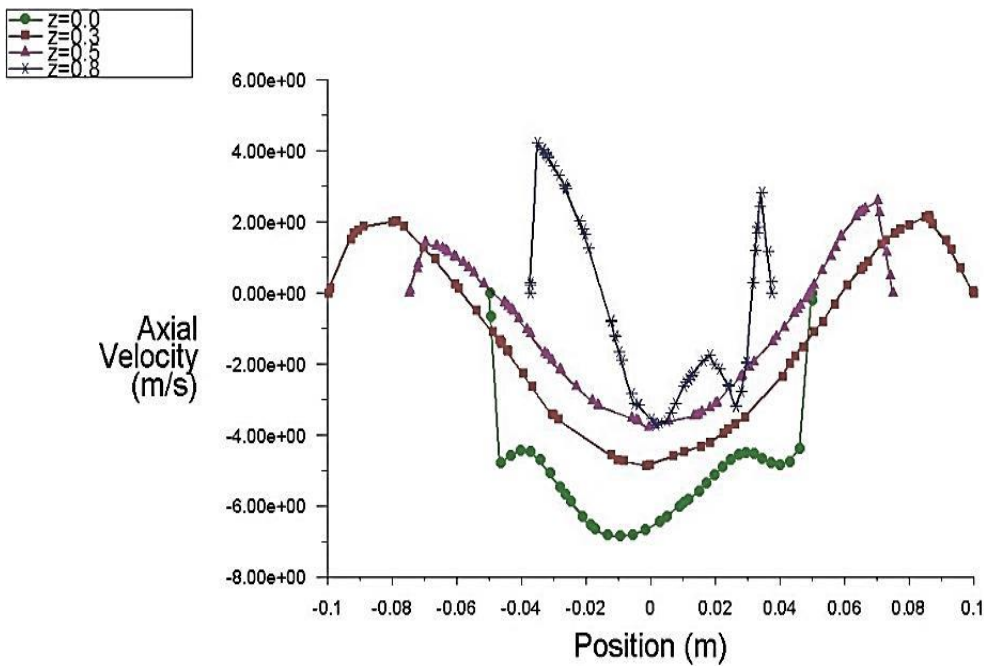


Fig. 8. Axial velocity at a series of vertical stations in a Stairmand cyclone at air inlet velocity of 10m/s

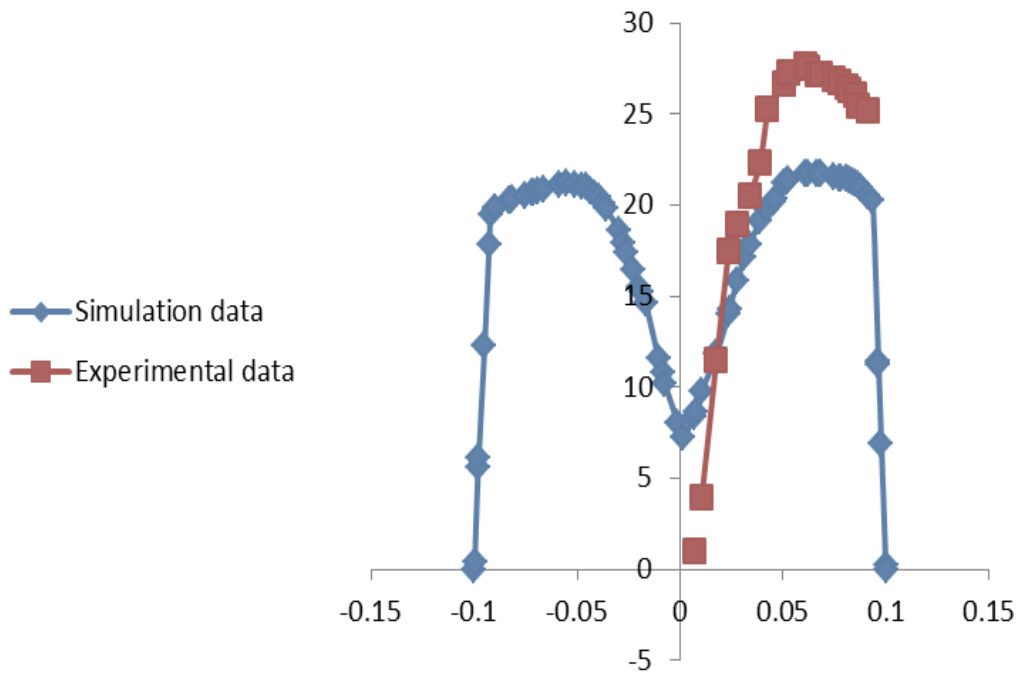


Fig. 9. The comparisons between Simulation data of Stairmand cyclone and experimental data in terms of tangential velocity at $Z=0.17\text{m}$

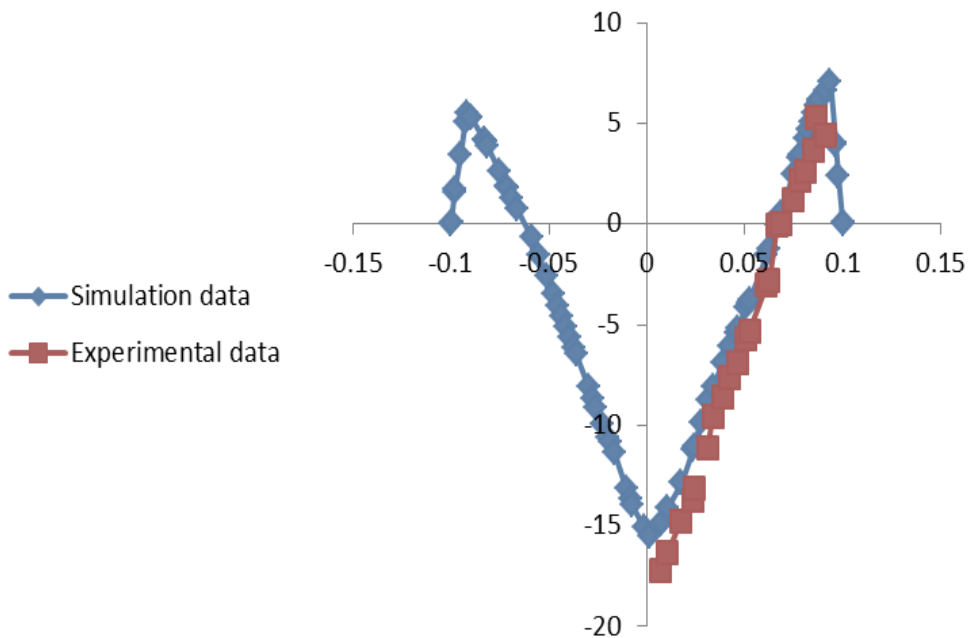


Fig. 10. The comparisons between simulation data of Stairmand cyclone and experimental data in terms of axial velocity at $Z=0.17\text{m}$

Pressure Field Behavior

Figure (11) shows that the contour of the static pressure at a vertical plane of a Stairmand cyclone at air inlet velocity of 10 m/s. It shows that the static pressure distribution decreased radially from the wall to the center of the cyclone. A low-pressure zone appeared in the center line of the cyclone due to high swirling velocity where a high-pressure zone appeared in the near wall region.

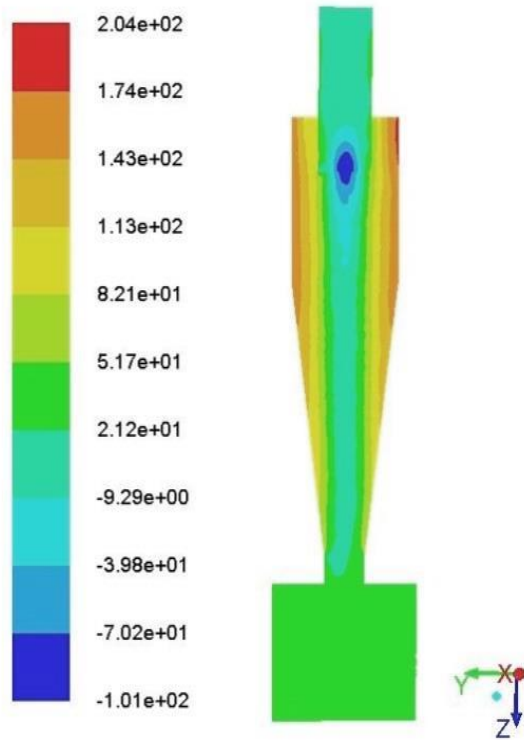


Fig. 11. Contour of static pressure at a vertical plane of Stairmand cyclone at air inlet velocity of 10m/s

Figure (12) shows the pressure drop profiles of Stairmand cyclone at different inlet velocities where the pressure drop increased with increasing the inlet air velocity. The highest pressure drop achieved at 15m/s which was 366.17Pascal where at 10m/s the pressure drop was 167.71Pascal and at 5m/s the pressure drop was only 40.65 Pascal.

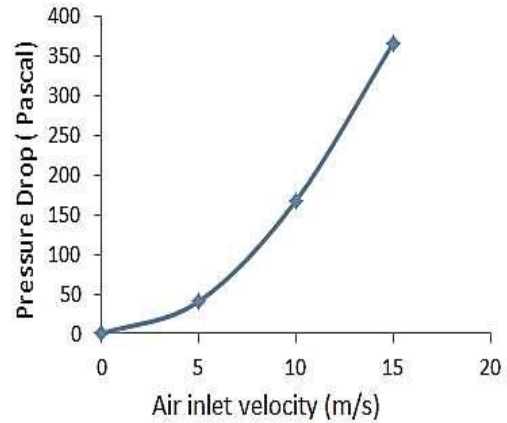


Fig. 12. Pressure drop vs. air inlet velocity of Stairmand cyclone

Particle Trajectories and Collection Efficiency

Figure (13) shows that the particles trajectories at the cyclone with different diameters size ranged as (5 – 200) μ m at inlet air velocity equal to 10m/s. Some particles in size (5–10) μ m were escaped from the cyclone while the other particles were collected. The particles at size greater than 80 μ m were still spinning near the wall at a certain horizontal level. This case was discussed briefly by Utikar et al.[2] and Wang et al. Wang [20], whom explain this phenomena as a critical value of the particle diameter which is the particles that not expected to be collected at the outlet.

The critical diameter in this cyclone was approximately 80 μ m. Figure (13) shows that when the particle diameter be larger than the critical diameter (>80 μ m), the particle will keep a circular motion in the cyclone body but when the particle diameter be less than the critical diameter (<80 μ m) the particles will be collected or escape from the cyclone.

The results of the collection efficiency, Figure (14), show that the efficiency increased as the particle diameter increased, and the collection efficiency of particle diameters less than 10 μ m was 93.71% and 100.00% of particle diameters larger than 10 μ m. It was found that the 50% cut size of this cyclone was approximately 4.3 μ m.

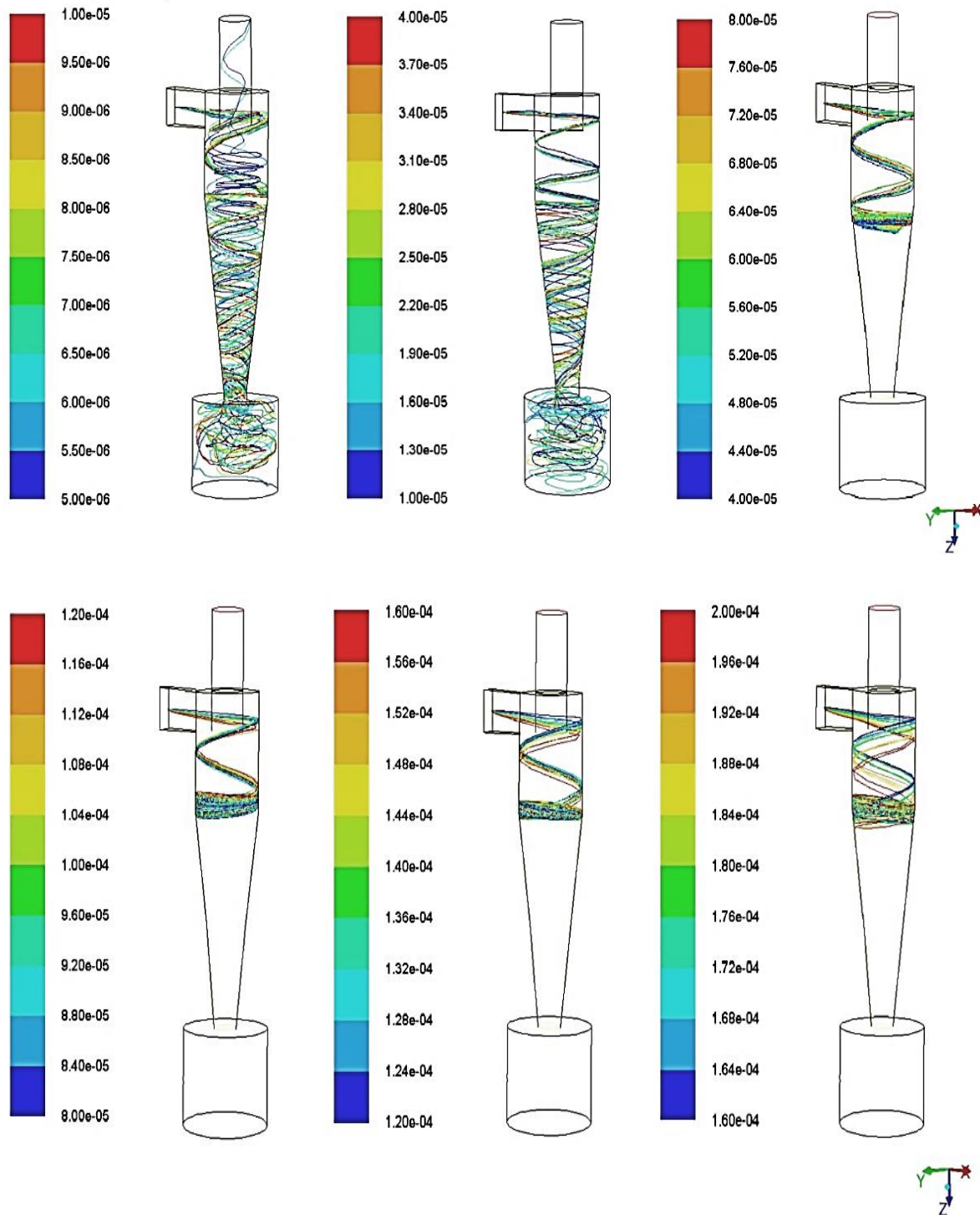


Fig. 13. The trajectories of particles with different diameters size ranged as (5–200) μm at Stairmand cyclone at inlet air velocity of 10 m/s

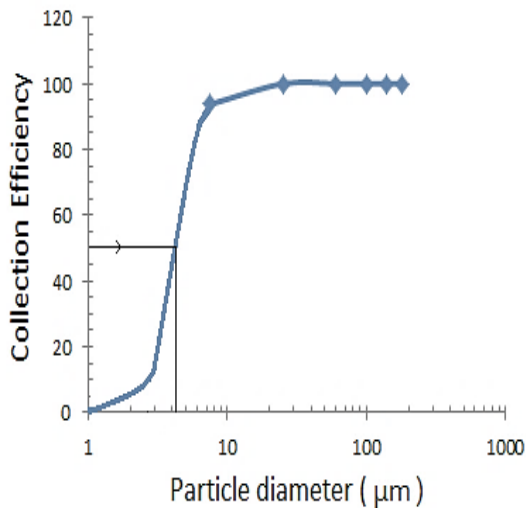


Fig. 14. The collection efficiency of Stairmand cyclone at air inlet velocity of 10m/s

Conclusions

The CFD code ANSYS FLUENT 14.5 with the RSM turbulence model, predicted very well the flow field parameters of cyclones and can be used in cyclone design for any dimensions. As well as the air flow behavior in cyclone separator consists of two vortices: an outer vortex with a downwardly directed axial flow and an inner vortex with an upwardly directed flow, this flow profile known as Rankine vortex. Also, the comparison between the simulation data gives a good agreement with experimental data with a deviation of 15% for tangential velocity and 10% for axial velocity from experimental data. The results showed that the static pressure distribution decreased radially from the wall to the center of the cyclone. Also, the results showed that the pressure drop increased with increasing the inlet air velocity. It was found that the collection efficiency of the studied cyclone increased as the particle diameter increased. The collection efficiency of the cyclone was 93.71% for particle diameters less than 10 μ m and 100.00% of particle diameters larger than 10 μ m. It was found that the 50% cut size of this cyclone was approximately 4.3 μ m.

References

- 1- Shukla S. K., Shukla P.a., Ghosh P., "Evaluation of Numerical Schemes using Different Simulation Methods for the Continuous Phase Modeling of Cyclone Separators", *Advanced Powder Technology*, Vol. 22, P. 209-219, 2011.
- 2- Utikar , R., Darmawan, N., Tade, M., Li, Q., Evans, G., and M.a.P. Glenn, V., "Hydrodynamic Simulation of Cyclone Separators, in *Computational Fluid Dynamics*", H.W. Oh, Editor., In Tech. p. 241-266, 2010.
- 3- Chuah L., Gimbut G., Thomas S. Y. Choong and A. Razi F., "A CFD Analysis on the Effect of Vortex Finder and Cylindrical Length on Cyclone Hydrodynamics and Centrifugal Forces", *The Institution of Engineers, Malaysia*, Vol. 71: p. 51-58, 2009.
- 4- Sinnott R. K., Coulson & Richardson's, "Chemical Engineering Chemical Engineering Design", Third ed., Vol. 6, Butterworth-Heinemann Oxford, 2003.
- 5- Sylvia N., Yunardi, Maulana I., Elwina, Wusnah and Bindar Y., "Analysis of Turbulence Models Performance for the Predictions of Flow Yield, Efficiency, and Pressure Drop of a Gas-solid Cyclone Separator", *Proceedings of The Annual International Conference Syiah Kuala University*, Vol. 1, p. 53-60, 2011.
- 6- Hoffmann A. C. and Stein L. E., "Gas Cyclones and Swirl Tubes ,Principles, Design and Operation", Second ed., Berlin Heidelberg New York, 2008.
- 7- Winfield D., Croft N., Paddison D., Craig I., "Performance Comparison of a Single and Triple Tangential Inlet Gas Separation Cyclone: A CFD Study", *Powder Technology*, Vol. 235, p. 520-531, 2013.
- 8- Cortes C., Gil A., "Modeling the Gas and Particle Flow Inside Cyclone Separators", *Progress in Energy and Combustion Science*, Vol. 33, p. 409-452, 2007.
- 9- Flagan R., Seinfeld J. H., "Fundamentals of Air Pollution Engineering", Prentice-Hall, Inc. A Division of Simon & Schuster, 1988.
- 10- Horvath A., C. J., Harasek M., "Influence of Vortex-Finder Diameter on Axial Gas Flow in Simple Cyclone", *Chemical Product and Process Modeling*, Vol. 3, p. 1-26, 2008.
- 11- Safikhani H. , Behabadi A. M. A. , Shams M. , Rahimyan M. H., "Numerical Simulation of Flow Field in Three Types of Standard Cyclone Separators", *Advanced Powder Technology*, Vol. 21, p. 435–442, 2010.

- 12- Andersson B., Andersson R., Hakansson L., Mortensen M., Sudiyo R., Wachem B., "Computational Fluid Dynamics for Engineers", First ed., USA, New York: Cambridge University Press, 2012.
- 13- Kegg, S., "A Numerical Investigation of Gas Cyclone Separation Efficiency with Comparison to Experimental Data and presentation of a Computer-based Cyclone Design Methodology", Thesis in Science, Akron, 2008.
- 14- ANSYS, I., ANSYS FLUENT Theory Guide, United States: ANSYS, Inc., 2012.
- 15- Martignoni W. P. , Bernardo S., Quintani C. L., "Evaluation of Cyclone Geometry and its Influence on Performance Parameters by Computational Fluid Dynamics (CFD)", Brazilian Journal of Chemical Engineering, Vol. 24, p. 83-94, 2007.
- 16- Elsayed K., "Optimization of the Cyclone Separator Geometry for Minimum Pressure Drop using Co-Kriging", Powder Technology, Vol. 269, p. 409-424, 2015.
- 17- Versteeg H. K., Malalasekera W., An Introduction to Computational Fluid Dynamics', The Finite Volume Method. First ed., United State: John Wiley & Sons Inc., 1995.
- 18- Jiyuan Tu, Yeoh G., Liu C., "Computational Fluid Dynamics", A Practical Approach. Second ed., USA: Elsevier Ltd., 2013.
- 19- Harwood R., Slack M., "CFD Analysis of a Cyclone", Fluent Europe Ltd, Sheffield, United Kingdom. QNET-CFD Network Newsletter, Vol. 1, p. 1-6, 2002.
- 20- Wang B., Xu D. L., Xiao G. X., Chu K. W., and Yu A. B., "Numerical Study of Gas-Solid Flow in a Cyclone Separator", Third International Conference on CFD in the Minerals and Process Industries , CSIRO, Melbourne, Australia, 2003.